NANO LETTERS

2008
Vol. 8, No. 10
3137-3140

Reduced Graphene Oxide Molecular Sensors

Jeremy T. Robinson,* F. Keith Perkins, Eric S. Snow,* Zhongqing Wei, and Paul E. Sheehan

Naval Research Laboratory, Washington, D.C. 20375

Received May 6, 2008; Revised Manuscript Received July 9, 2008

ABSTRACT

We demonstrate reduced graphene oxide as the active material for high-performance molecular sensors. Sensors are fabricated from exfoliated graphene oxide platelets that are deposited to form an ultrathin continuous network. These graphene oxide networks are tunably reduced toward graphene by varying the exposure time to a hydrazine hydrate vapor. The conductance change of the networks upon exposure to trace levels of vapor is measured as a function of the chemical reduction. The level of reduction affects both the sensitivity and the level of 1/*f* noise. The sensors are capable of detecting 10 s exposures to simulants of the three main classes of chemical-warfare agents and an explosive at parts-per-billion concentrations.

Molecular detection using fullerene nanomaterials—i.e., sp^2-bonded carbon structures of single atomic layer thickness—is a promising area of nanotechnology. Fullerenes are relatively inexpensive, thermally and chemically stable, come in a variety of different geometries (spheres, tubes, and sheets), can be grown and processed with high precision, and are generally process-compatible with conventional microlithographic techniques. Moreover, because every atom in a fullerene is a surface atom, electron transport through these materials can be highly sensitive to adsorbed molecules. This phenomenon has subsequently enabled the fabrication of sorption-based sensors capable of detecting trace levels of vapor using conventional low-power electronics.

To date, the most successful such efforts are built upon single-walled carbon nanotubes (SWNTs), where the sensing transduction mechanism is based upon changes in conductance[1,2] (due to charge transfer or mobility change) or capacitance[3] (from intrinsic or induced dipole moments) when a molecular species interacts with the SWNT sidewalls. Though exact details of the interaction chemistry remain elusive, it is clear that molecular interactions with defect sites in SWNT sidewalls can dominate their electrical response,[4] that the interactions of a molecule with a sp^2-bonded carbon site differ dramatically from those with a high-energy defect site, and that controlling the defect density can enhance sensor sensitivity and specificity.[4] However, the optimal defect density will balance the gains in sensitivity against the rapid degradation in conductivity due to the defects. In this regard graphene oxide (GO)—a graphene sheet decorated with oxygen functional groups[5]—is an ideal material for balancing these effects because it contains a diverse range of surface sites whose density is easily controlled.

Here we report the fabrication and characterization of molecular sensors based on reduced graphene oxide thin-film networks. Graphene oxide is a chemically modified graphene[6] containing oxygen functional groups such as epoxides, alcohols, and carboxylic acids,[7] and chemical analysis shows the carbon to oxygen ratio to be approximately three to one.[8] Recently, GO has received a great deal of attention because it readily exfoliates as single sheets in water and, from these solutions, it is straightforward to produce continuous films.[9−12] This affords GO a distinct advantage over fullerenes which are typically deposited as films by use of high temperatures and vapor transport and should allow the use of plastic substrates or other temperature-sensitive processes.

In its as-oxidized state the numerous oxygen functional groups of GO render it too electrically insulating for use as a conductance-based sensor; however, chemical reduction using hydrazine hydrate vapor can restore the conductivity several orders of magnitude[9] by removal of oxygen and recovery of aromatic double-bonded carbons. Even so, this process does not repair the material to pure graphene—at least some oxygen groups remain after long exposures to hydrazine. Thus, reduced graphene oxide (rGO) is both conductive and has chemically active defect sites making it a promising candidate for the active material in molecular sensors. Here we show this material readily allows the detection of chemical agents in the parts-per-billion range with significantly reduced noise levels over carbon nanotube-based sensors.

* Corresponding authors. E-mail: J.T.R., jeremy.robinson@nrl.navy.mil; E.S.S., snow@bloch.nrl.navy.mil.

10.1021/nl8013007 CCC: $40.75
Published on Web 09/03/2008

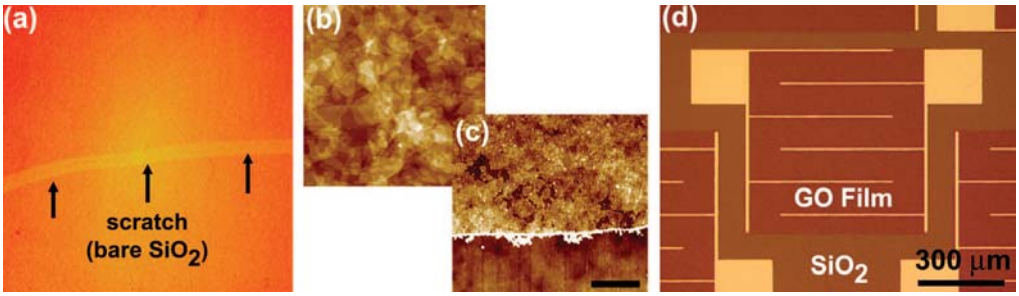

Figure 1. (a) Optical microscope (OM) image (20×) showing a uniform graphite oxide film on a 250 nm SiO_2/Si substrate that was deposited via spin-casting. A scratch has been made across the sample to reveal a slight color contrast between the uniform film averaging 2 nm and the substrate. (b) Atomic force microscopy (AFM) image showing the film is composed of single overlapping GO platelets. Platelet thickness is quantized at ~1 nm. (c) AFM image showing the boundary of a GO film after photolithographically processing devices from the film (z = 6 nm, scale bar = 1 μm). (d) OM image showing an electrically isolated GO device with interdigitated Ti/Au contacts.

Forming these ultrathin GO thin films requires a few simple steps. First, GO powder is created using the widely reported Hummers[13] method. This powder is resuspended in a solution of methanol and water, centrifuged to remove large residual particles, and then cast onto a thermally oxidized Si substrate spinning at 4000 rpm with nitrogen simultaneously blown over the sample to increase solvent evaporation. Film thickness is controlled by varying either the concentration of GO platelets in solution (0.5 mg/mL to 3.0 mg/mL), or the volume of solution during spin-casting—typically 50−100 μL deposited onto a 25 × 25 mm^2 substrate for the thinnest continuous films. This technique results in large-area, continuous films absent of nanometer scale wrinkling found in other GO deposition procedures[11] (Figure 1b,c). Before additional processing the GO films are heated in argon to 150 °C for 15 min to remove residual solvent and water. Standard photolithography is then used to create interdigitated arrays of Ti/Au electrodes with finger spacings ranging between 10 and 340 μm (Figure 1d). Processed samples are subsequently reduced back toward graphene by exposure to a hydrazine hydrate vapor up to 24 h while being heated to 100 °C.

To test the sensor response of these reduced graphene oxide devices we exposed them to 5 s pulses of dilute acetone vapor in air while simultaneously measuring the relative change in electrical conductance ($\Delta G/G_o$). We note that the response observed for acetone is typical of most of the vapors we have tested. Figure 2a shows a comparison of the real-time conductance response of a GO device reduced for 17 h in hydrazine vapor to the conductance response of a SWNT network device[14] of similar total area to increasing concentrations of acetone vapor. Analysis of the curves in Figure 2a can be broken into two parts—the "rapid" (steep slope) and "slow" (shallow slope) response. The rapid response arises from molecular adsorption onto low-energy binding sites, such as sp^2-bonded carbon, and the slow response arises from molecular interactions with higher-energy binding sites, such as vacancies, structural defects, and oxygen functional groups. Adsorption on sp^2-bonded carbon occurs through weak dispersive forces, while at a defect such as a carboxylic acid group single- and double-hydrogen bonding allows binding energies of at least several hundred meV/molecule.[4] As is evident from Figure 2a, the

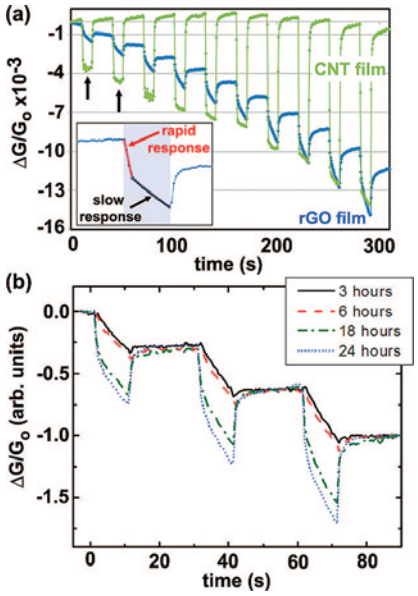

Figure 2. (a) Real-time conductance response to 5 s acetone pulses of increasing concentration for a SWNT network sensor (light green) and a rGO network sensor (blue). Arrows on the plot mark the first two of ten pulses, which increase in concentration from P/P_o = 0.025% to P/P_o = 1%, where P_o is the vapor pressure of acetone. Inset: close-up of the fifth pulse highlighting the "rapid" and "slow" response of the rGO device. (b) Plot of the normalized conductance response to 5 s pulses of acetone for GO devices reduced with hydrazine for 3, 6, 18, and 24 h. With increasing reduction time the fast response increases while the slow response decreases.

rapid response is recoverable, whereas the slow response is generally nonrecoverable without moderate heating, and leads to integration of the conductance signal.

The striking difference between the rapid and slow response of the SWNT and rGO device is perhaps not surprising because the intrinsic concentration of oxygen defects on SWNTs is quite low. On the other hand, the almost one-to-one ratio between the rapid and slow response of the rGO devices is a direct reflection of the remnant high-energy adsorption sites after incomplete reduction. Because oxygen defects can play a dominant role in the sensor characteristics of SWNTs, we expect oxygen defect density to heavily influence the conductance response of the rGO material as well. To systematically study this, we expose GO devices to hydrazine hydrate vapor for different times, thereby

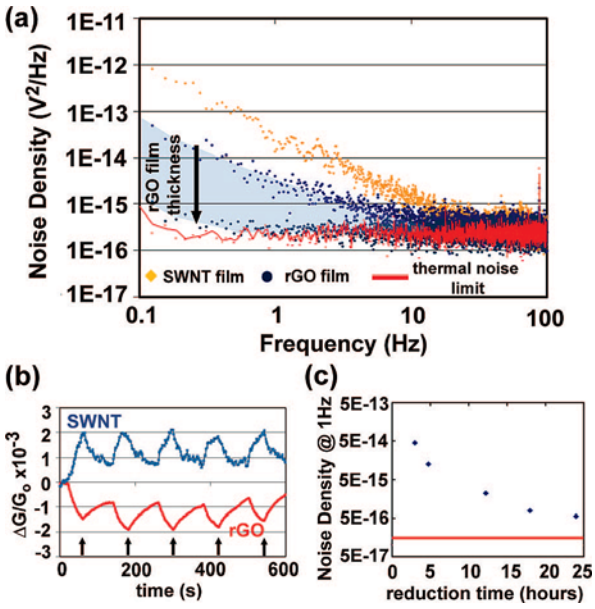

Figure 3. (a) Noise density spectrum for SWNT and rGO devices. The top (light orange) curve shows the low-frequency noise response of a SWNT sensor which follows a well-known 1/*f* behavior below 10 Hz. The blue (lower) curves show the noise response of a 2 and 4 nm rGO sensor. Depending on rGO film thickness, the noise response can be tuned (shaded area) to the thermal noise limit of the instrumentation, shown by the solid red curve. (b) Conductance response ($\Delta G/G_o$) of a SWNT and rGO device to 30 s pulses of 0.5 ppb DNT (dinitrotoluene). Arrows mark the end of each 30 s pulse. (c) Plot of noise density at 1 Hz vs hydrazine reduction time for GO films with the same thickness. The red line marks the thermal noise limit.

changing the oxygen defect density. Figure 2b shows normalized responses to acetone for GO devices reduced at different intervals. A clear trend is observed in the response—with increasing reduction time the rapid response increases and the slow response decreases. This is consistent with the fact that the number of sp^2-bonded carbon sites increases while at the same time the higher-energy adsorption sites (i.e., oxygen functional groups) decrease.

To date, the temporal evolution of GO chemistry during hydrazine reduction remains vague. After long exposures the oxygen to carbon ratio is reduced from approximately 1:3 to 1:10. In these samples it has also been found that ~25% of the rGO carbons remain functionalized.[8] Reaction mechanisms[5] and FT-IR measurements[15] suggest carboxyl groups make up the largest portion of these unreduced groups, though epoxides and alcohols are undoubtedly present as well. From the data shown in Figure 2b we can only make general statements about surface chemistry due to the range in remnant oxygen functional group types, as well as density. It is clear, however, that hydrazine reduction is a knob with which to tune the sensing response of GO-based devices. Further experiments are underway to deconvolute the affect of specific oxygen functional groups on the conductance response of sp^2 carbon-based sensors.

When chemical sensor performance is considered, there are two important parameters. As discussed above, one of these parameters is the sensitivity of the conductance response to molecular adsorbates. The second significant consideration is the low-frequency noise, which is generally dominated by 1/*f* noise. The 1/*f* noise arises from fluctuations in carrier mobility[16] or carrier density[17] and is ubiquitous in solid-state devices.[18] In the case of SWNTs such fluctuations can arise from trapped charges in the oxide[16,17] or the presence of defects within individual tubes. Interestingly, it was recently shown[19] that 1/*f* noise in bilayer graphene is strongly suppressed compared to nanotubes even in the presence of similar oxides. An effective screening of charge fluctuations from external impurity charges is identified as the root of this difference.

Such screening could explain the 10−100 fold reduction in 1/*f* noise in our rGO sensors over SWNT-based sensors, as shown in Figure 3a. This figure compares the low-frequency noise density spectrum of a SWNT device and two rGO devices and reveals that the noise level in rGO devices strongly decreases with increasing film thickness. The shaded region of Figure 3a shows the noise variation as film thickness is varied from an average of 2 to 4 nm. Films over 4 nm consistently show noise response at the thermal noise limit of the experimental setup. The increase in charge carrier number from a 2 nm to a 4 nm film would not be expected to decrease the noise 10-fold and suggests that impurity charge screening is further reducing 1/*f* noise. Figure 3b demonstrates the important role of noise reduction by comparing the responses of SWNT and rGO devices to 0.5

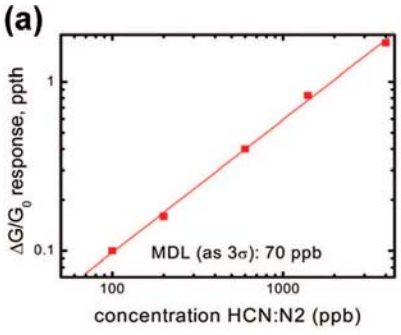

(b)

Simulant	SWNT: 10 s (ppb)	rGO: 10 s (ppb)	JCAD specifications [22] ≤ 10 s (ppb)	CDC specifications [23] (ppb)
HCN	>4,000	70	$2x10^6$	$5x10^4$ [a]
CEES	0.5	0.5	7,500	0.5 [b]
DMMP	0.1	5	170	17 [a]
DNT	0.1	0.1	——	——

[a] Immediately Dangerous to Life or Health (IDLH): ≤ 30 minutes does not cause death
[b] Threshold Limit Value (TLV): lifetime exposure without adverse health risk

Figure 4. (a) Response of a rGO sensor to decreasing levels of hydrogen cyanide (HCN). (b) Comparison of the minimum detectable level (MDL) for a SWNT network sensor and a rGO network sensor to 10 s pulses of HCN, CEES,[24] DMMP,[24] and DNT, as well as the targeted response to live agents according to specifications for the JCAD detector[22] and exposure limits provided by the CDC.[23] For the CDC exposure limits, the IDLH values are defined as a concentration that for up to 30 min does not cause death, serious or irreversible health effects, or does not impair or impede the ability to escape. The TLV values are defined as a concentration a worker can be exposed day after day for a working lifetime without adverse health effects.

ppb 2,4-dinitrotoluene (DNT), a simulant for the explosive TNT. The lower noise levels in the rGO device lead to a notable increase in signal-to-noise ratio.

The extent of chemical reduction also affects low-frequency noise. Films exposed to hydrazine vapor for longer times show reduced 1/*f* noise, as revealed in Figure 3c. (Note that this trend is also observed for the curves shown in Figure 2b). As the GO material is reduced back toward graphene there is a large increase in film conductivity. In turn this leads to a reduction in noise levels of rGO devices.

The benchmark for chemical sensors is the minimal detectable level (MDL), which comprises both the sensor response due to adsorption and the device noise level. For SWNT sensors the lowest MDLs are realized in a capacitance-based measurement mode[20] due to reduced 1/*f* noise. Therefore, we use the SWNT capacitance response MDLs as a basis of comparison here. Figure 4b compares the MDLs achieved for capacitance-based SWNT sensors[14] and conductance-based rGO sensors to 10 s exposures[21] to simulants of an explosive and the three main classes of chemical warfare agents—blood, blister, and nerve agents. In addition, we also compare the target specifications of a portable detector for military applications, called The Joint Chemical Agent Detector (JCAD),[22] as well as exposure limits set by the Center for Disease Control (CDC).[23]

Figure 4a shows the normalized response $\Delta G/G_o$ of an rGO device to 10 s doses of increasing concentration of hydrogen cyanide (HCN) in nitrogen. The MDL is defined here as that concentration of vapor which gives rise to a change in conductance ΔG that is exactly three standard deviations from G_o (i.e., a signal-to-noise ratio of three). Assuming a linear response function, we find the MDL is 70 ppb. For SWNTs we are unable to detect HCN at the highest concentration tested (4000 ppb) in our experimental setup. For other simulants such as CEES[24] and DNT we find comparable MDLs between rGO conductance-based and SWNT capacitance-based detection, whereas the MDL for DMMP[24] is an order of magnitude lower for SWNT sensors (Figure 4b). We note these results highlight how different classes of molecules can distinctly interact with different surface sites—HCN weakly interacts with nominally pristine sp^2-bonded nanotubes while strongly interacting with remnant defects in rGO; the reverse is true for organophosphates (i.e., DMMP), and the responses to aromatics and alkane derivatives are similar (i.e., DNT and CEES, respectively). Thus, these two carbon-based nanomaterials can provide complimentary capabilities of chemical agent detection and further stress the importance of tailoring surface chemistry to enhance sensitivity. Identification of specific oxygen functional groups that interact strongly with each simulant should allow even lower MDLs for rGO-based sensors.

In conclusion, we have demonstrated reduced graphene oxide as a promising active material for molecular sensors. Reduced graphene oxide devices readily achieve sensitivities at parts-per-billion levels for both chemical warfare agents and explosives. The response and recovery characteristics of the conductance response can be tailored by adjusting the reduction process. Moreover, the low-frequency noise of graphene oxide devices is sensitive to both hydrazine hydrate exposure time, as well as film thickness, and is orders of magnitude lower than SWNT-based sensors. Finally, the relatively large number of chemically active oxygen defects affords the possibility of covalent chemical functionalization for increased chemical or biological selectivity.

Acknowledgment. This research was performed while J. T. Robinson and Z. Wei held a National Research Council Research Associateship Award at the Naval Research Laboratory.

References

(1) Collins, P. G.; Bradley, K.; Ishigami, M.; Zettl, A. *Science* **2000**, *287* (5459), 1801–1804.
(2) Kong, J.; Franklin, N. R.; Zhou, C.; Chapline, M. G.; Peng, S.; Cho, K.; Dai, H. *Science* **2000**, *287* (5453), 622–625.
(3) Snow, E. S.; Perkins, F. K.; Houser, E. J.; Badescu, S. C.; Reinecke, T. L. *Science* **2005**, *307* (5717), 1942–1945.
(4) Robinson, J. A.; Snow, E. S.; Badescu, S. C.; Reinecke, T. L.; Perkins, F. K. *Nano Lett.* **2006**, *6* (8), 1747–1751.
(5) Stankovich, S.; Dikin, D. A.; Piner, R. D.; Kohlhaas, K. A.; Kleinhammes, A.; Jia, Y.; Wu, Y.; Nguyen, S. T.; Ruoff, R. S. *Carbon* **2007**, *45* (7), 1558–1565.
(6) Ruoff, R. *Nat. Nano* **2008**, *3* (1), 10–11.
(7) Lerf, A.; He, H.; Forster, M.; Klinowski, J. *J. Phys. Chem. B* **1998**, *102* (23), 4477–4482.
(8) Stankovich, S.; Piner, R. D.; Chen, X.; Wu, N.; Nguyen, S. T.; Ruoff, R. S. *J. Mater. Chem.* **2006**, *16* (2), 155–158.
(9) Gilje, S.; Han, S.; Wang, M.; Wang, K. L.; Kaner, R. B. *Nano Lett.* **2007**, *7* (11), 3394–3398.
(10) Wang, X.; Zhi, L.; Mullen, K. *Nano Lett.* **2008**, *8* (1), 323–327.
(11) Becerril, H. A.; Mao, J.; Liu, Z.; Stoltenberg, R. M.; Bao, Z.; Chen, Y. *ACS Nano* **2008**, *2* (3), 463–470.
(12) Eda, G.; Fanchini, G.; Chhowalla, M. *Nat Nano* **2008**, *3* (5), 270–274.
(13) Hummers, W.; Offeman, R. *J. Am. Chem. Soc.* **1958**, *80*, 1339.
(14) Snow, E. S.; Perkins, F. K. *Nano Lett.* **2005**, *5* (12), 2414–2417.
(15) Li, D.; Muller, M. B.; Gilje, S.; Kaner, R. B.; Wallace, G. G. *Nat. Nano* **2008**, *3* (2), 101–105.
(16) Ishigami, M.; Chen, J. H.; Williams, E. D.; Tobias, D.; Chen, Y. F.; Fuhrer, M. S. *Appl. Phys. Lett.* **2006**, *88* (20), 203116–3.
(17) Lin, Y. M.; Appenzeller, J.; Knoch, J.; Chen, Z.; Avouris, P. *Nano Lett.* **2006**, *6* (5), 930–936.
(18) Hooge, F. N. *IEEE Trans. Electron Devices* **1994**, *41*, 1926.
(19) Lin, Y.-M.; Avouris, P. *Nano Lett.* **2008**, *8* (8), 2119–2125.
(20) Snow, E. S.; Perkins, F. K.; Robinson, J. A. *Chem. Soc. Rev.* **2006**, *35*, 790–798.
(21) Ten seconds is the fastest target response time set by The Joint Chemical Agent Detector (JCAD) program.
(22) Laljer, C. E. Joint Chemical Agent Detector (JCAD): The Future of Chemical Agent Detection, 11th Annual US Army Ground Vehicle Survivability Symposium, March 27−30, 2000.
(23) Center for Disease Control and Prevention. http://www.bt.cdc.gov/agent/, 2008.
(24) Chloroethylethyl sulfide (CEES) is a simulant for sulfur mustard gas; dimethylmethylphosphonate (DMMP) is a simulant for sarin.

NL8013007